

Fundamentals of Theoretical Organic Chemistry

Lecture 3.

1.2 Theoretical Background

The evolution of Theoretical Organic chemistry covers a long stretch of time. Before large scale competitions became feasible qualitative orbital pictures were used to rationalize certain chemical phenomena. The material covered in the following section may be found in textbooks but not at a single volume rather they are scattered all over the literature.

1.2.1 Early orbital concepts for the description of saturated and unsaturated compounds

Quantum Chemistry

The application of Quantum Mechanics to chemical problems is normally referred to as Quantum Chemistry. The birth of quantum mechanics created a revolution in physics during the first third of the 20th century. In the last third of the 20th century, the numerical implementation of the principles of quantum mechanics to chemical problems, which is now called computational chemistry, has created a similar revolution in chemistry, particularly in organic chemistry. This revolutionary change is expected to continue and increase in the 21st century.

In almost every freshman chemistry textbook it is well explained that the Schrödinger equation

$$H\Psi = E\Psi$$

1.2.1-1. eq.

of the H-atom, or of H - like ions (He^+ , Li^{2+} , Be^{3+} , B^{4+} ,...etc.), is a one-electron wave equation which can be solved analytically. The solutions of the Schrödinger equation are the atomic orbitals of the H - atom (or H - like ions) and the associated orbital energies ($E = \epsilon$). Atomic orbitals are mathematical functions. For example, the 1s orbital for H has the following form

$$\Psi_{1s} = \chi_{1s} = \frac{1}{\sqrt{\pi}} e^{-r}$$

1.2.1-2. eq.

where r is the distance of the electron measured from the atomic nucleus, i.e. from the proton. A mathematical solution is possible because in a one-electron system, all of the state wave functions are one-electron functions, or "orbitals". In many electron atoms (e.g. Be) however, the solutions of the corresponding many-electron Schrödinger equations are more complicated. In general, they are constructed from one-electron wave functions, i.e., from orbitals. In the case of Be, the 4 - electron state-wave function is constructed as two doubly occupied atomic orbitals (χ_{1s} and χ_{2s}) in which the double occupancy is stipulated to involve one electron with α spin and one with β spin.

$$\psi(1,2,3,4) \sim \underbrace{\chi_{1s}(1)\alpha(1)\chi_{1s}(2)\beta(2)}_{1s^2} \underbrace{\chi_{2s}(3)\alpha(3)\chi_{2s}(4)\beta(4)}_{2s^2} \Rightarrow 1s^2 2s^2$$

1.2.1-3. eq.

This double occupancy is frequently denoted in terms of the energy levels ϵ_{1s} and ϵ_{2s} .

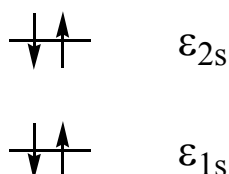


Figure 1.2.1—1. Orbital energy level diagram for Be showing double occupancy.

Similarly, for the 10 electron Ne atom the 10 electron state-wave function $\Psi(1,2, \dots, 9, 10)$ is constructed from five doubly occupied atomic orbitals (χ_{1s} , χ_{2s} , χ_{2p_x} , χ_{2p_y} , χ_{2p_z}) corresponding to the mathematically rigorous form of the $1s^2 2s^2 2p^6$ occupancy scheme (c.f. Figure 1.2.1—2).

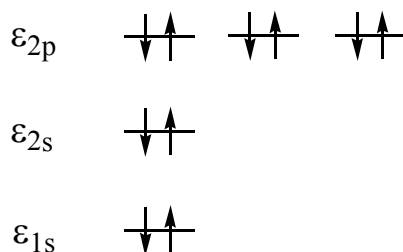


Figure 1.2.1—2 Orbital energy level diagram for Ne showing double occupancy

The situation for many-electron molecular systems is analogous to that of many-electron atoms; i.e. the many-electron state wave functions are constructed from many one-electron wave functions. But, though one-centered atomic orbitals were appropriate in the case of atoms multicentered one-electron functions, i.e. molecular orbitals are necessary in the case of molecules (c.f. Figure 1.2.1—2).

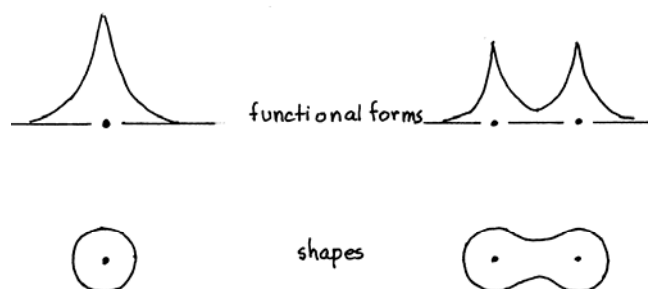


Figure 1.2.1—3 One-centered one-electron functions, i.e. atomic orbitals (AO) on the left, and multi-centered one-electron functions, i.e. molecular orbitals (MO) on the right.

Molecular orbitals are constructed by the linear combination of atomic orbitals (LCAO). Consider the $2p_z$ atomic orbital for carbon (c.f. Figure 1.2.1—3) where α is the orbital exponent and N is the normalization constant:

$$\chi_{2p_z} = Nze^{-\alpha r}$$

1.2.1-4. eq.

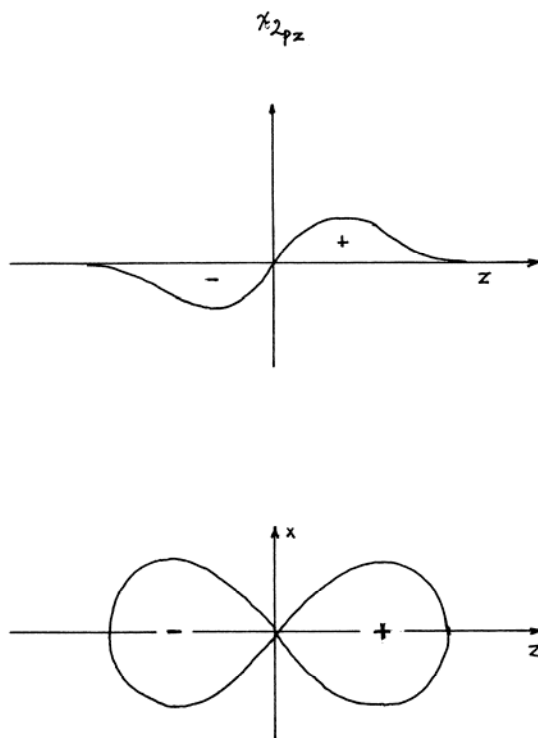


Figure 1.2.1—4 The functional form (above) and the shape (below) of a $2p_z$ atomic orbital. The + and - represent the sign of the mathematical function denoted by χ_{2p_z} .

Two types of MO can be constructed from a pair of $2p$ type AO's depending on their orientations; a σ - type and a π - type, as illustrated by Figure 1.2.1—4. An axial orientation yields a σ - bonding and a σ^* anti-bonding orbital pair, while a parallel orientation yields a π - bonding and a π^* anti-bonding orbital pair.

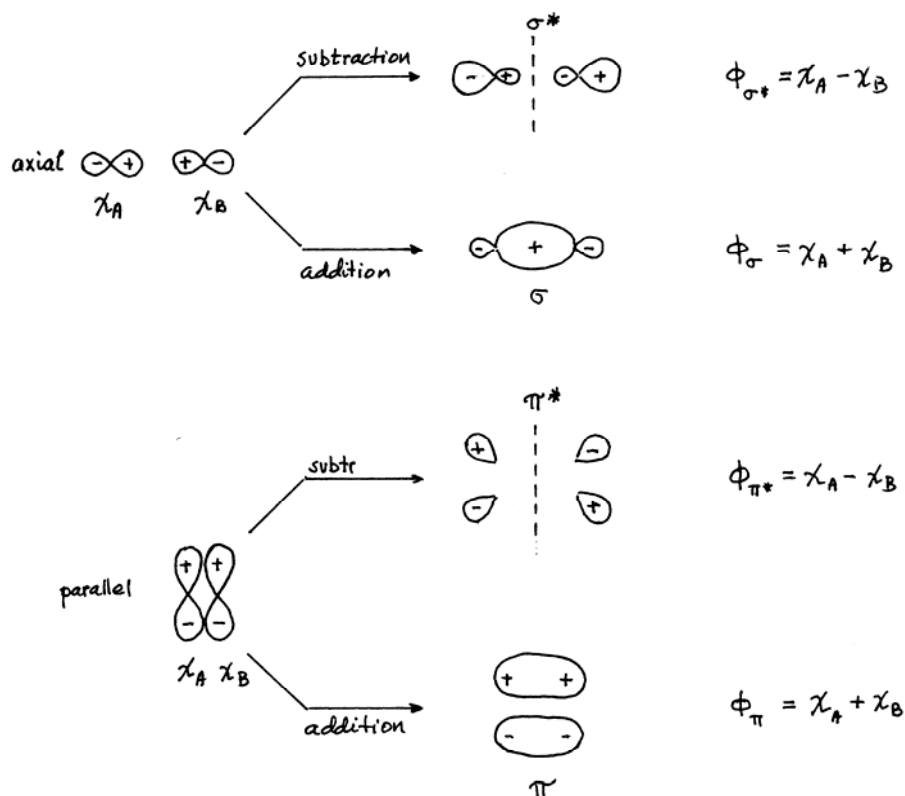


Figure 1.2.1—5. Two symmetrical types (σ and π) of molecular orbitals in bonding (σ and π) and antibonding (σ^* and π^*) arrangements. The axial arrangement leads to σ and σ^* and the parallel arrangement leads to π and π^* orbitals.

Figure 1.2.1—5 illustrates the Linear Combination of Atomic Orbitals (LCAO). Linear combination is a mathematical process of Linear Algebra where vectors are subjected to linear combination i.e. multiplication with weighing coefficients and subsequent addition and/or subtraction. In this sense, atomic orbitals may be regarded as vectors. This is obvious in the case of p_x , p_y and p_z orbitals (c.f. Figure 1.2.1—6.)

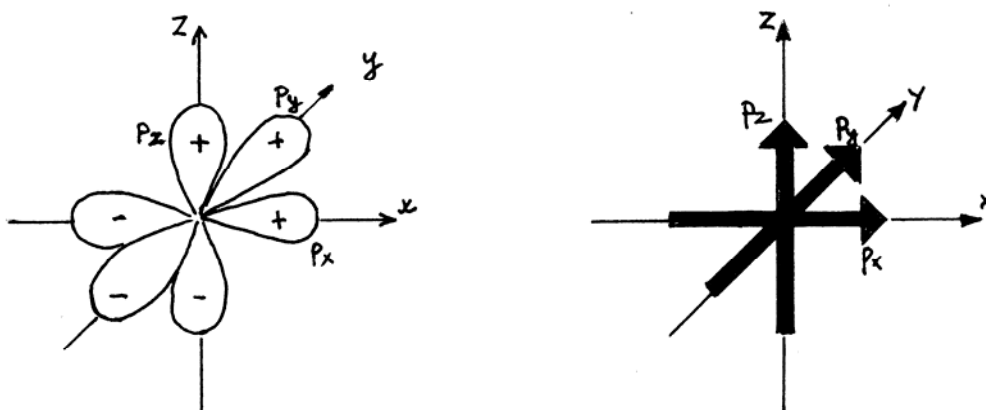
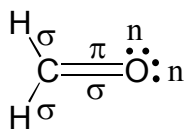


Figure 1.2.1—6. A schematic representation of shape (A) and a vector model (B) of the 2p atomic orbitals.

Although 1s and 2s orbitals have no directionality like $2p_x$, $2p_y$ and $2p_z$ orbitals, they can also be regarded as vectors. Thus, the electron distribution for C, N, O, F, and Ne may be represented by 5 vectors, 1s, 2s, $2p_x$, $2p_y$, $2p_z$. These five vectors will be part of the so-called 'basis vectors' or 'basis sets' for a molecular orbital calculation. For a general molecule, such as formaldehyde, the MO description involves both σ and π molecular orbitals:



1.2.1-5. eq.

Furthermore, one must account for the 16 electrons that correspond to 8 doubly occupied MO's. One may recognize 2 atomic cores (i.e. $1s^2$ for C and $1s^2$ for O), 3 σ - bonds (a C - O and two C - H bonds), 2 n - type lone electron pairs (lp) and 1 π - electron pair. In addition to these 7 σ and 1 π double occupied MO's, there are a number of empty (antibonding or virtual) MO's. These MO's may be correlated with the AO's of the component atoms. The atomic orbital basis set consists of a grand total of 12 AO's which are transformed to 12 MO's (eight doubly occupied and four empty). (Figure 1.2.1—7).

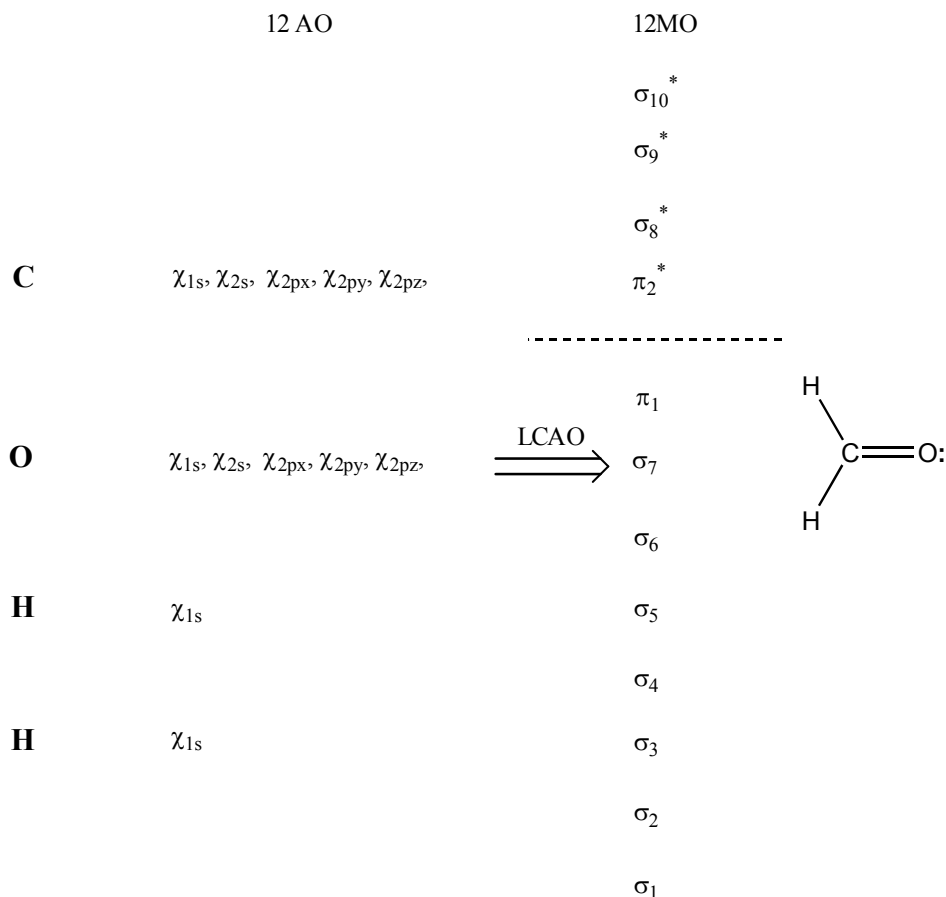


Figure 1.2.1—7 The LCAO transformation of the 12 AO basis set to 12 MO, eight of which are doubly occupied and four of which are empty (denoted by *). Core electron pairs are also σ type.

These 12 AO represent the 'basis set' for the MO calculation for formaldehyde. Figure 1.2.1—8 shows a schematic correlation of the orbital energies before and after the LCAO calculation.

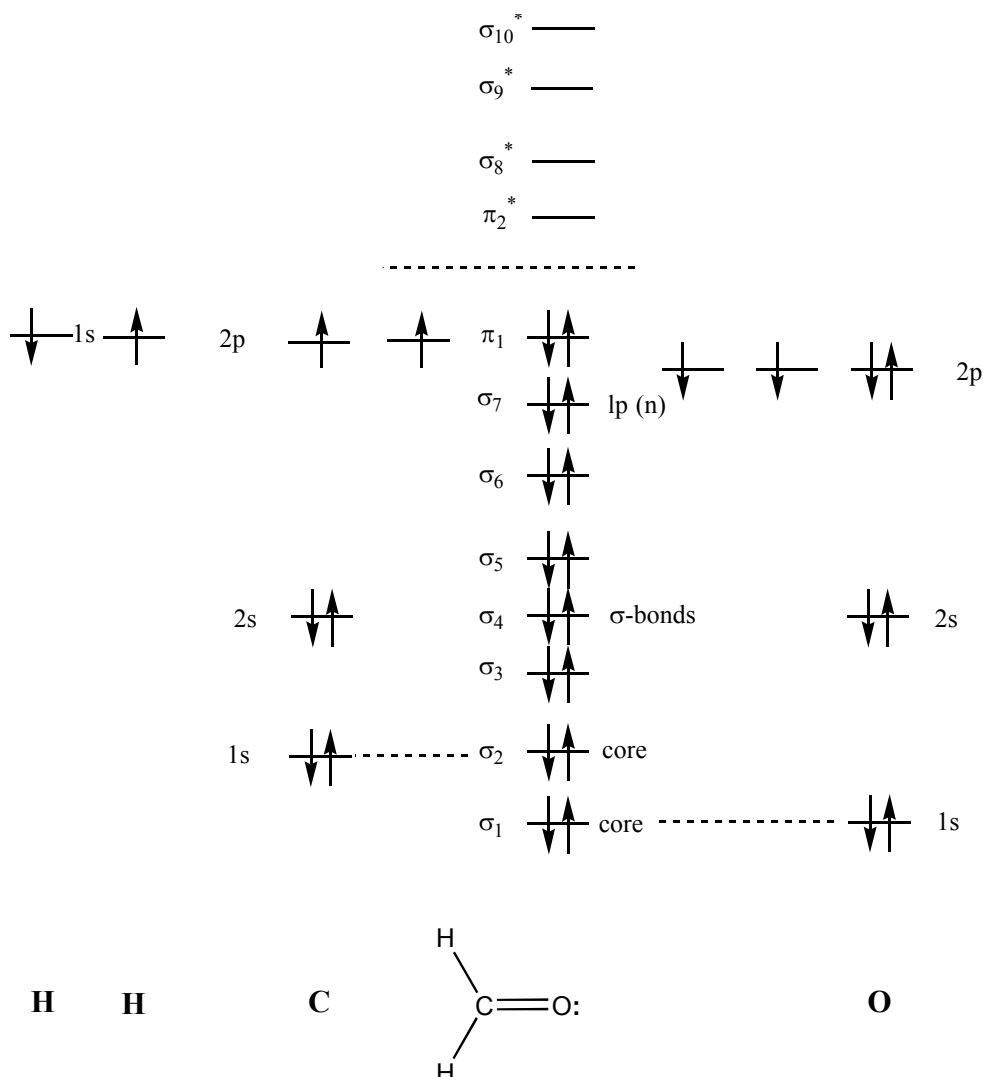


Figure 1.2.1—8 Schematic correlation of AO and MO energy levels for formaldehyde. In this energy level diagram, the highest occupied molecular orbital (HOMO) is π_1 the lowest unoccupied molecular orbital (LUMO) is π_2^*

The set of MO's obtained from the LCAO-MO calculation reflects the symmetry of the molecule. These MO's are called canonical MO's (CMO's); they are fully delocalized and they are not directed along the traditional representation of chemical bonds.

For further discussion, let us consider a simple molecule like H₂O. Here too, the CMO's obtained from the LCAO calculation do not correspond to two equivalent bonds directed along the O - H lines. Instead, a symmetric and an anti-symmetric delocalized σ -type CMO, are obtained. However, the linear combination (i.e. addition and subtraction) of these CMO's leads to localized molecular orbitals (LMO's) which show the directionality of the two O - H bonds.

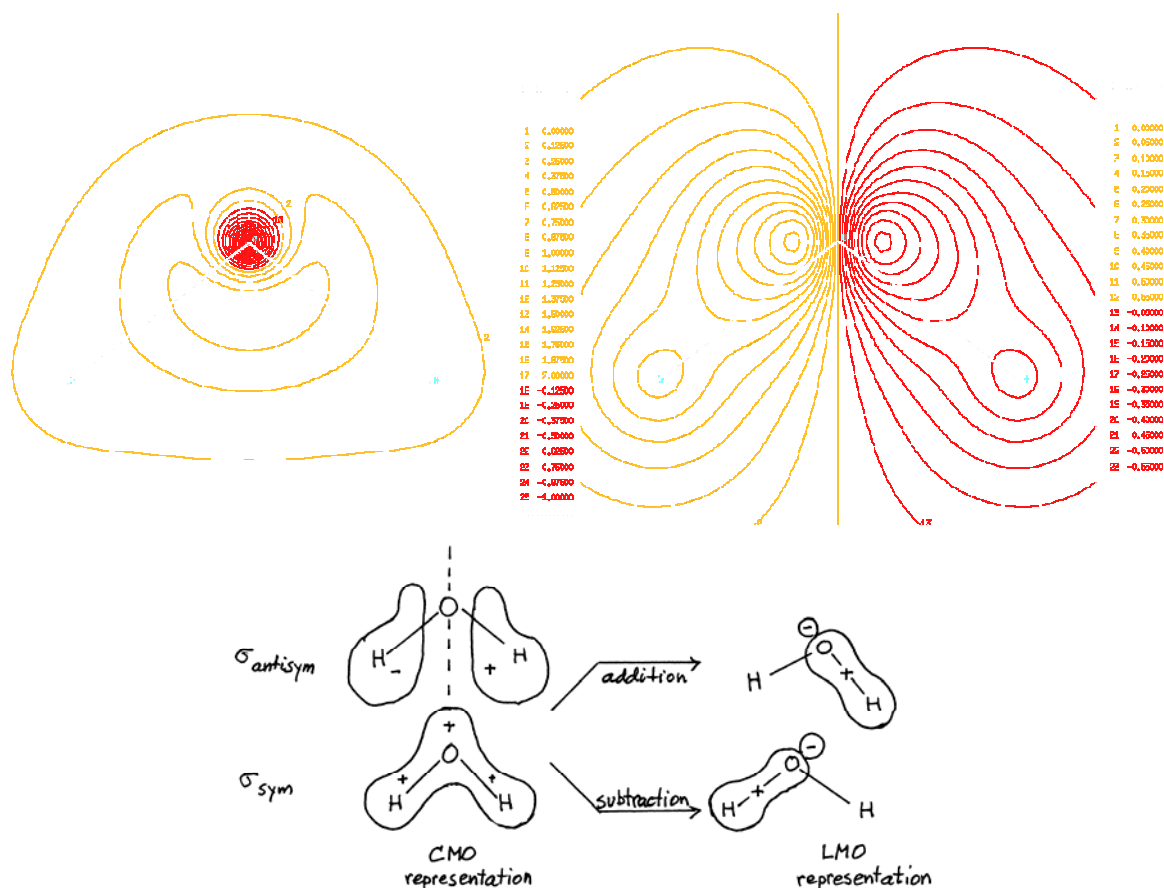


Figure 1.2.1—9 A schematic illustration of the two equivalent (CMO and LMO) representations and the associated transformations of the two bonding σ -type molecular orbitals (MO) describing the two O - H bonds of H_2O .

The CMO representations of molecules have many advantages (e.g. they are directly computable from the AO basis set and they faithfully represent the symmetry of the molecule) but they have one disadvantage: they do not have a directionality, which coincides with the direction of the chemical bonds. The $2s$ AO has no directionality and the $2p_x$, $2p_y$ and $2p_z$ AO's show the directionality of an arbitrarily chosen Cartesian (x , y , z) coordinate system. This directionality need not necessarily match the variety of structural features organic molecules exhibit.

If we were to catalogue the various structural motifs organic molecules can have, we would find no more than three motifs. These are shown in Figure 1.2.1—10. These three structural motifs have characteristic bond angles and an increasing number of ligands ($2 \rightarrow 3 \rightarrow 4$).

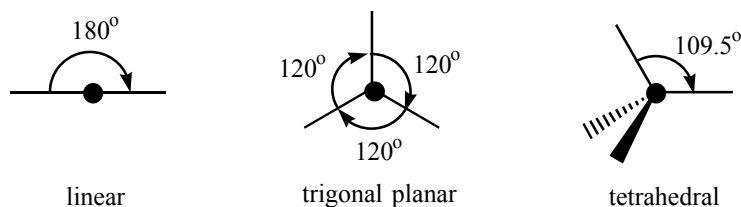


Figure 1.2.1—10 The three most important structural motifs in organic chemistry.

Clearly, the Cartesian coordinates do not match all three structural motifs. Even though, the directionality of the AO is not a prerequisite for the formation of a MO, for a qualitative or pictorial description of bonding, chemists frequently hybridize the Cartesian AO. As a result, chemical problems are often discussed in terms of hybrid atomic orbitals (HAO). This process of hybridization corresponds to an orthogonal transformation of a given basis set ($\chi_1 = 2s$; $\chi_2 = 2p_x$; $\chi_3 = 2p_y$; $\chi_4 = 2p_z$) to an equivalent basis set $\{\lambda_i\}$. Since the hybridization may involve the mixing (i.e. linear combination) of two ($2s, 2p_x$), three ($2s, 2p_x, 2p_y$) or four ($2s, 2p_x, 2p_y, 2p_z$) AO's, it is possible to derive 3 types of hybridization, referred to as sp , sp^2 and sp^3 respectively. The mathematical relationships that define these three sets of HAO's and the corresponding vector models are shown in Figure 1.2.1 -11 can be derived under the condition that both the original set of AOs and the set of hybrid AOs are orthonormal (they are each normalized and they are orthogonal to each other). The approximate shape of carbon sp , sp^2 and sp^3 orbital is shown in Figure 1.2.1—12

The computed CMO's are delocalized over the whole molecule whether they belong to the σ or the π representations. Also, the CMO's are symmetry adapted. On the other hand, the geometrical equivalents of localized molecular orbitals (LMO) are governed by the stereochemistry of the molecular bonding. Methane may be used to illustrate this point.

Neglecting the core electrons of methane, we have to account for 8 electrons or 4 electron pairs, which require 4 MO's. In the CMO description, a totally symmetrical MO (a_1 type), showing no orientation, and a triply degenerate MO (t - type), oriented towards the x , y and z directions (t_x, t_y, t_z), are obtained. These are illustrated in Figure 1.2.1—13

In the CMO representation, the molecular orbital levels have triply degenerate energy values and a somewhat lower value associated with a_1 . On the other hand the "orbital - energy" value associated with the LMO basis has four-fold degeneracy because each of the 4 C-H bonds is equivalent (cf. Figure 1.2.1—14).

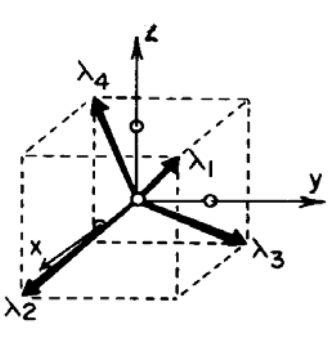
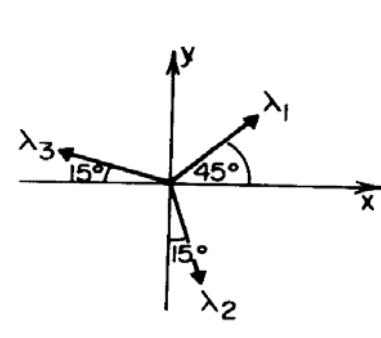
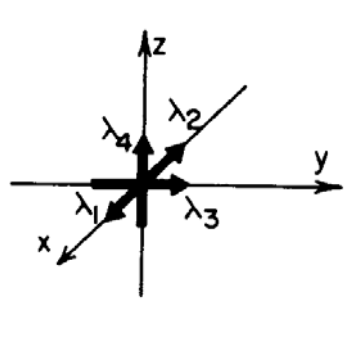
sp^3 hybrids	sp^2 hybrids	sp hybrids
$\lambda_1 = \frac{1}{2}(\chi_1 + \chi_2 + \chi_3 + \chi_4)$ $\lambda_2 = \frac{1}{2}(\chi_1 + \chi_2 - \chi_3 - \chi_4)$ $\lambda_3 = \frac{1}{2}(\chi_1 - \chi_2 + \chi_3 - \chi_4)$ $\lambda_4 = \frac{1}{2}(\chi_1 - \chi_2 - \chi_3 + \chi_4)$	$\lambda_1 = 1/\sqrt{3}(\chi_1 + \chi_2 + \chi_3)$ $\lambda_2 = 1/\sqrt{3}(\chi_1 + 0.366\chi_2 - 1.366\chi_3)$ $\lambda_3 = 1/\sqrt{3}(\chi_1 - 1.366\chi_2 + 0.366\chi_3)$ $\lambda_4 = \chi_4$	$\lambda_1 = 1/\sqrt{2}(\chi_1 + \chi_2)$ $\lambda_2 = 1/\sqrt{2}(\chi_1 - \chi_2)$ $\lambda_3 = \chi_3$ $\lambda_4 = \chi_4$
		

Figure 1.2.1—11 Vector model and analytical expressions of the three most commonly used HAOs.

In the case of sp^2 , the unhybridized $\chi_4 = 2p_z$ is specified as λ_4 . In the case of sp , the unhybridized $\chi_3 = 2p_y$ and $\chi_4 = 2p_x$ are denoted as λ_3 and λ_4 .

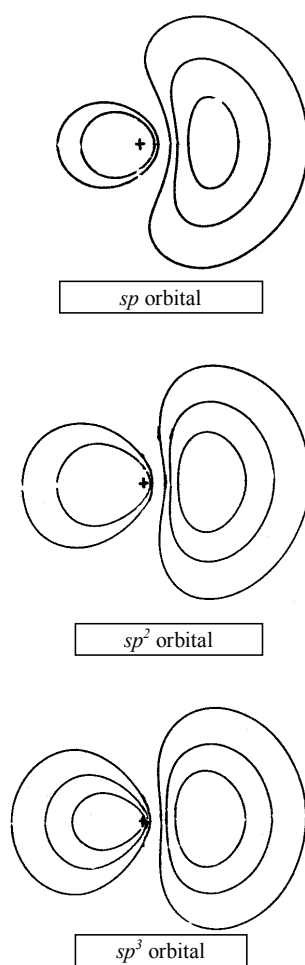


Figure 1.2.1—12 Approximate shapes of sp , sp^2 and sp^3 hybrid atomic orbitals (HAO) of carbon.

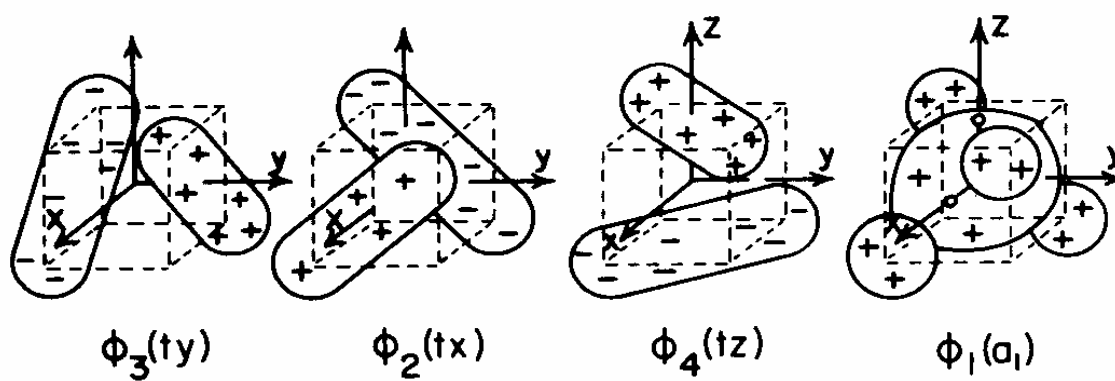


Figure 1.2.1—13 A schematic representation of the shapes and orientation of the four valence CMO of CH_4 .

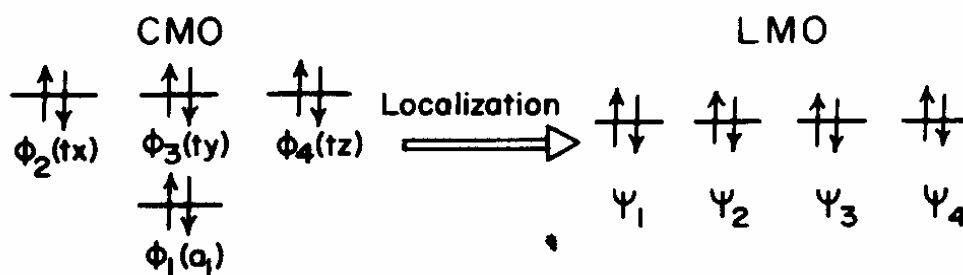
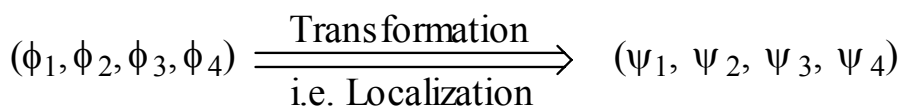


Figure 1.2.1—14. A schematic representation of the change of energy levels upon localization.

The "localization" referred to in Figure 1.2.1—15 is a transformation from the CMO basis set to the LMO basis set. Just as it was illustrated for the two bonding molecular orbitals in the case of H₂O in Figure 1.2.1—9, this involves the addition or subtraction of the four ϕ (CMO) to obtain the four ψ (LMO)



1.2.1-6. eq.

The four LMO's must be derived by localization in such a way that each is directed along a C - H bond, as indicated schematically in Figure 1.2.1—15

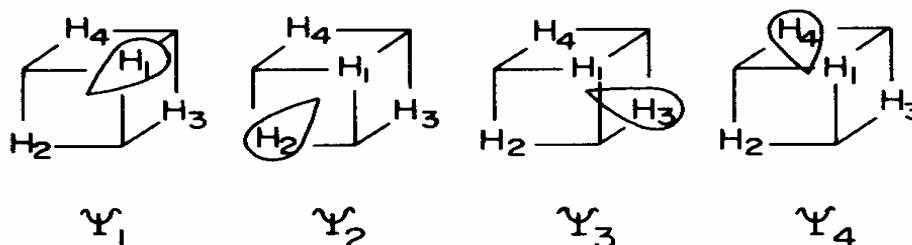


Figure 1.2.1—15 A schematic representation of the shapes and orientation of the four valence LMO of CH₄ obtained by localization of the four valence CMO's.

For CH₄, the four C - H bonds { Ψ_1 }, may also be formed from the four sp³ hybrid AO { λ_i } and the 1s orbitals { χ_{Hi} } of the four hydrogen atoms, as illustrated in Figure 1.2.1—16.. The wave functions are shown in 1.2.1-7. eq..

$$\begin{aligned}\psi_1 &= a\lambda_1 + b\chi_{H1} \\ \psi_2 &= a\lambda_2 + b\chi_{H2} \\ \psi_3 &= a\lambda_3 + b\chi_{H3} \\ \psi_4 &= a\lambda_4 + b\chi_{H4}\end{aligned}$$

1.2.1-7. eq.

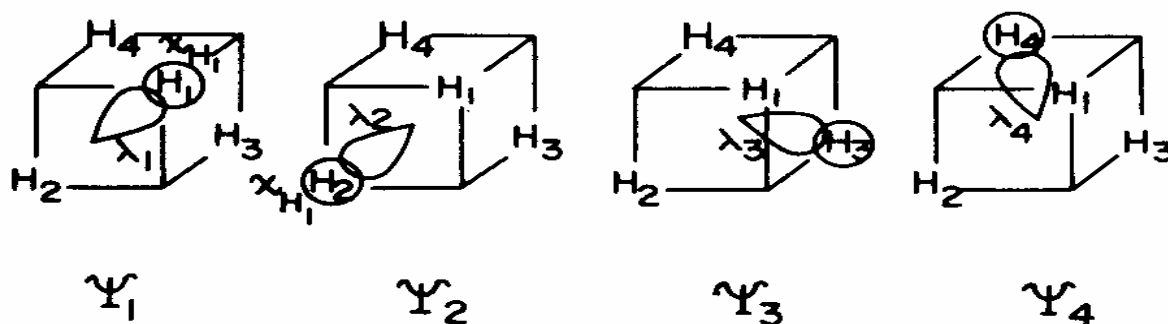


Figure 1.2.1—16. A schematic representation of the linear combination of carbon HAO and hydrogen AO to form methane LMO.

However, $\{\lambda_i\}$, the HAOs also have their own expression in terms of the unhybridized AO of carbon. Take for example the first of the series ψ_1 (remember that $\chi_1 = 2s$, $\chi_2 = 2p_x$, $\chi_3 = 2p_y$, $\chi_4 = 2p_z$ and $\chi_{H1} = 1s_{H1}$).

$$\Psi_1 = a(\chi_1 + \chi_2 + \chi_3 + \chi_4) + b(\chi_{H1})$$

1.2.1-8. eq.

In order to see the set of ψ (LMO) expressed in terms of the AO (cf. Figure 1.2.1—9) we have to specify the expressions for the set of ϕ (CMO). The shapes and orientation of these CMO have been shown previously (c.f. sp^3 in Figure 1.2.1-11) and are given below in 1.2.1-9. eq..

$$\begin{aligned}\phi_1 &= C_1\chi_1 + C_2(\chi_{H1} + \chi_{H2} + \chi_{H3} + \chi_{H4}) \\ \phi_2 &= C_1\chi_2 + C_2(\chi_{H1} - \chi_{H2} + \chi_{H3} - \chi_{H4}) \\ \phi_3 &= C_1\chi_3 + C_2(\chi_{H1} - \chi_{H2} - \chi_{H3} + \chi_{H4}) \\ \phi_4 &= C_1\chi_4 + C_2(\chi_{H1} + \chi_{H2} - \chi_{H3} - \chi_{H4})\end{aligned}$$

1.2.1-9. eq.

Let us examine ψ_1 , the first LMO, only. The first LMO (ψ_1) may be written as the following linear combination of the four CMO: ϕ_1 , ϕ_2 , ϕ_3 and ϕ_4 .

$$\begin{aligned}\psi_1 &= \frac{1}{2}\phi_1 + \frac{1}{2}\phi_2 + \frac{1}{2}\phi_3 + \frac{1}{2}\phi_4 \\ &= \frac{1}{2}\{\phi_1 + \phi_2 + \phi_3 + \phi_4\} \\ &= \frac{1}{2}\{C_1\chi_1 + C_2(\chi_{H1} + \chi_{H2} + \chi_{H3} + \chi_{H4}) \\ &\quad + C_1\chi_2 + C_2(\chi_{H1} - \chi_{H2} + \chi_{H3} - \chi_{H4}) + C_1\chi_3 + C_2(\chi_{H1} - \chi_{H2} - \chi_{H3} + \chi_{H4}) \\ &\quad + C_1\chi_4 + C_2(\chi_{H1} + \chi_{H2} - \chi_{H3} - \chi_{H4})\}\end{aligned}$$

1.2.1-10. eq.

When the addition is performed, the terms involving χ_{H2} , χ_{H3} and χ_{H4} cancel and we are left with the expression

$$\Psi_1 = C_1\left\{\frac{1}{2}(\chi_1 + \chi_2 + \chi_3 + \chi_4)\right\} + 2C_2\chi_{H1}$$

1.2.1-11. eq.

The hybrid structure is clearly recognizable (cf. Figure 1.2.1—8) in the first term of the above, expression and we may rewrite it conveniently in the form

$$\Psi_1 = C_1\lambda_1 + 2C_2\lambda_{H1}$$

1.2.1-12. eq.

This may now be compared to the equation given at the beginning of this section for the first LMO, i.e. one of the C - H,

$$\Psi_1 = a_1\lambda_1 + b_1\chi_{H1}$$

1.2.1-13. eq.

Thus, the CMO and LMO representations are equivalent.

Consider H₂O again. The LMO picture of the 4 valance electron pairs related to an sp³ hybridized oxygen is given schematically in Figure 1.2.1—17. The two lone electron pairs (lp) point to the back and the two bond pairs (O - H) point towards the front. The two bond pairs have been discussed earlier in this chapter (Figure 1.2.1—8).

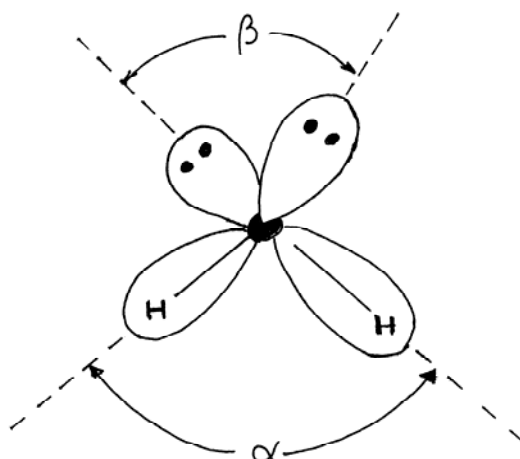


Figure 1.2.1—17. Localized molecular orbitals (LMO) for the water molecule. In the ideal case $\alpha = 109.5^\circ = \beta$; in reality $\alpha < 109.5^\circ < \beta$.

It was shown in Figure 1.2.1—8 that the CMO and LMO representations of the two O-H bond pairs are equivalent. It is now illustrated in Figure 1.2.1—18. that the CMO and LMO representations of the two lone pairs are also equivalent. Both representations lead to the same 4 lone-pairs electron density, just as both CMO and LMO representations of the two bond pairs give the same 4-bond electron density. As shown schematically in Figure 1.2.1—19, the plane containing the 2 lone-pairs is perpendicular to the plane containing the 2 bond pairs.

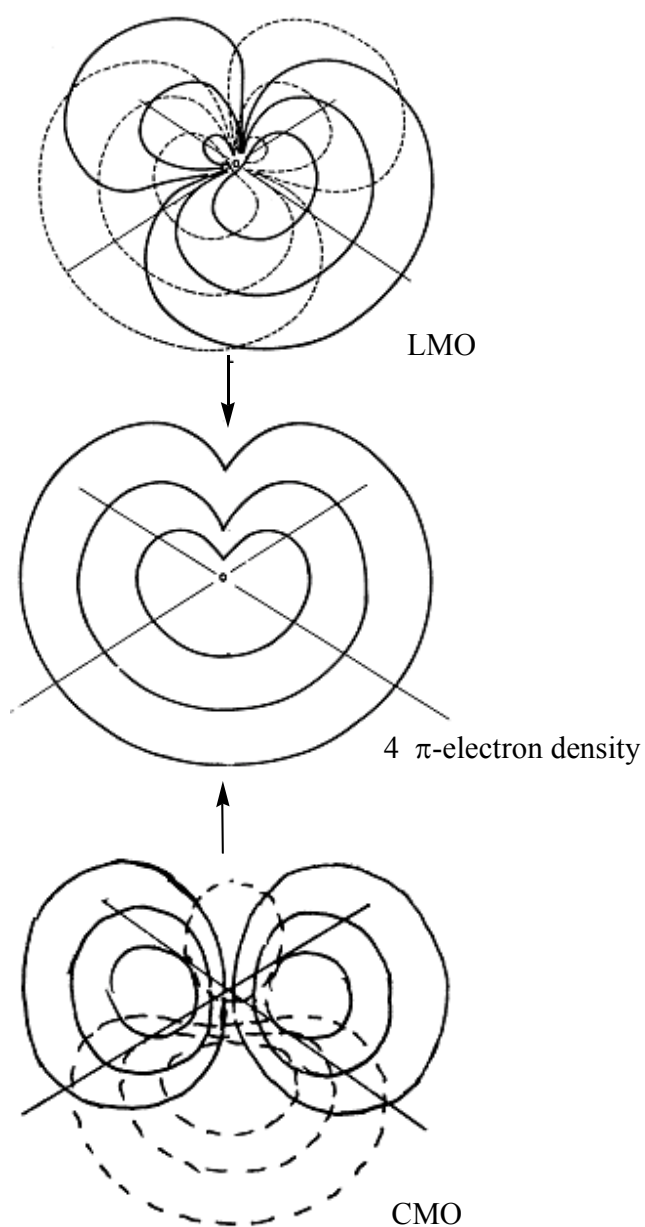


Figure 1.2.1—18. A schematic illustration of the fact that both LMO and CMO representations of the 2 lone pairs of oxygen in H_2O lead to the same 4-electron density.

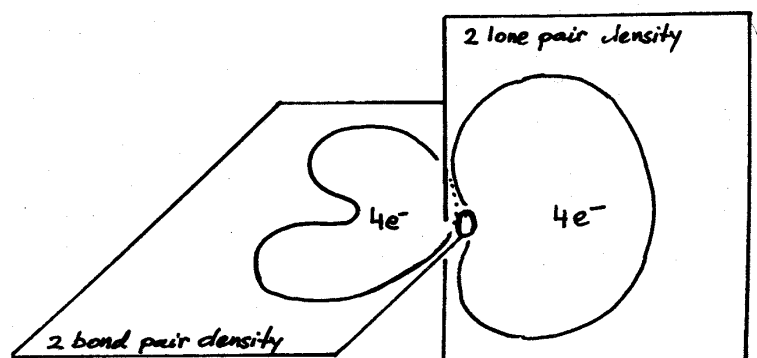
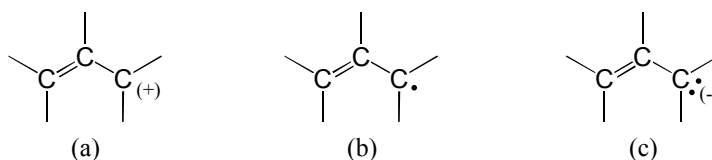


Figure 1.2.1—19 Two orthogonal planes containing the 4 bond electron density and the 4 lone-pair electron density.

Molecular Orbital (MO) Description of the Allyl Cation, Radical and Anion

The following molecular structures are associated with the allyl cation (1.2.1-14. eq. a), allyl radical (1.2.1-14. eq. b) and allyl anion (1.2.1-14. eq. c).



1.2.1-14. eq.

These are planar structures with 120° bond angles. Thus, each of the carbon atoms may be regarded as sp^2 hybridized, which means that each of the carbon atoms has an unhybridized $2p_z$ atomic orbital perpendicular to the plane of the molecule. This is shown in Figure 1.2.1—20

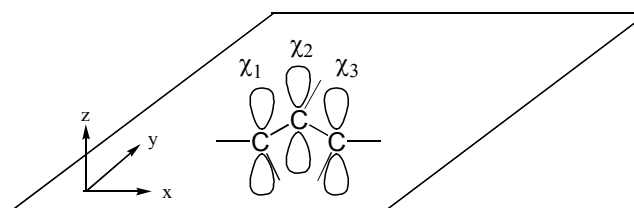


Figure 1.2.1—20 A schematic illustration of the geometry of the allyl system showing the three unhybridized $2p_z$ orbitals (χ_j) from which the π -type molecular orbitals (ϕ_i) are constructed by the LCAO method.

There are various levels of quantum chemical methods, which can be used to quantify orbital theory, but the simplest of all is the method developed by Hückel in 1931, the Hückel Molecular Orbital (HMO) Theory or, the Simple Hückel Molecular Orbital (SHMO) Theory as it is now called. Later, Professor R. Hoffmann introduced the Extended Hückel Molecular Orbital (EHMO) method, which can be used to study organic reactions. In 1981, Professor Hoffmann received the Nobel Prize for his development of the EHMO method.

The transformation of atomic orbitals (AOs), denoted by χ , to molecular orbitals (MOs) or canonical molecular orbitals (CMOs), both denoted by Φ , is known as the Linear Combination of Atomic Orbitals (LCAO) method. For the allyl system, three AOs (χ_1, χ_2, χ_3) are combined to form three MOs or CMOs (Φ_1, Φ_2, Φ_3), which correspond to the following equations:

$$\phi_1 = 0.500\chi_1 + 0.707\chi_2 + 0.500\chi_3$$

1.2.1-15. eq.

$$\phi_2 = 0.707\chi_1 - 0.707\chi_3$$

1.2.1-16. eq.

$$\phi_3 = 0.500\chi_1 - 0.707\chi_2 + 0.500\chi_3$$

1.2.1-17. eq.

If we regard the set of ϕ_i and the set of χ_j as vectors, the transformation may be written in linear algebra notation as

$$\begin{pmatrix} \phi_1 \\ \phi_2 \\ \phi_3 \end{pmatrix} = \begin{pmatrix} 0.500 & 0.707 & 0.500 \\ 0.707 & 0.000 & -0.707 \\ 0.500 & -0.707 & 0.500 \end{pmatrix} \begin{pmatrix} \chi_1 \\ \chi_2 \\ \chi_3 \end{pmatrix}$$

1.2.1-18. eq.

Denoting the coefficient matrix in equation 1.2.1-18. eq. as \mathbf{C} , the equation may be rewritten in an abbreviated form as equations 1.2.1-19. eq. or 1.2.1-20. eq., where ϕ and χ are regarded as vectors, with χ being the basis vector or basic set of the expansion.

$$\phi = \mathbf{C}\chi$$

1.2.1-19. eq

$$\phi_i = \sum_{j=1}^3 c_{ij}\chi_j$$

1.2.1-20. eq.

Figure 1.2.1—21. shows the shape of the CMOs in a schematic fashion. Broken lines denote the nodal planes.

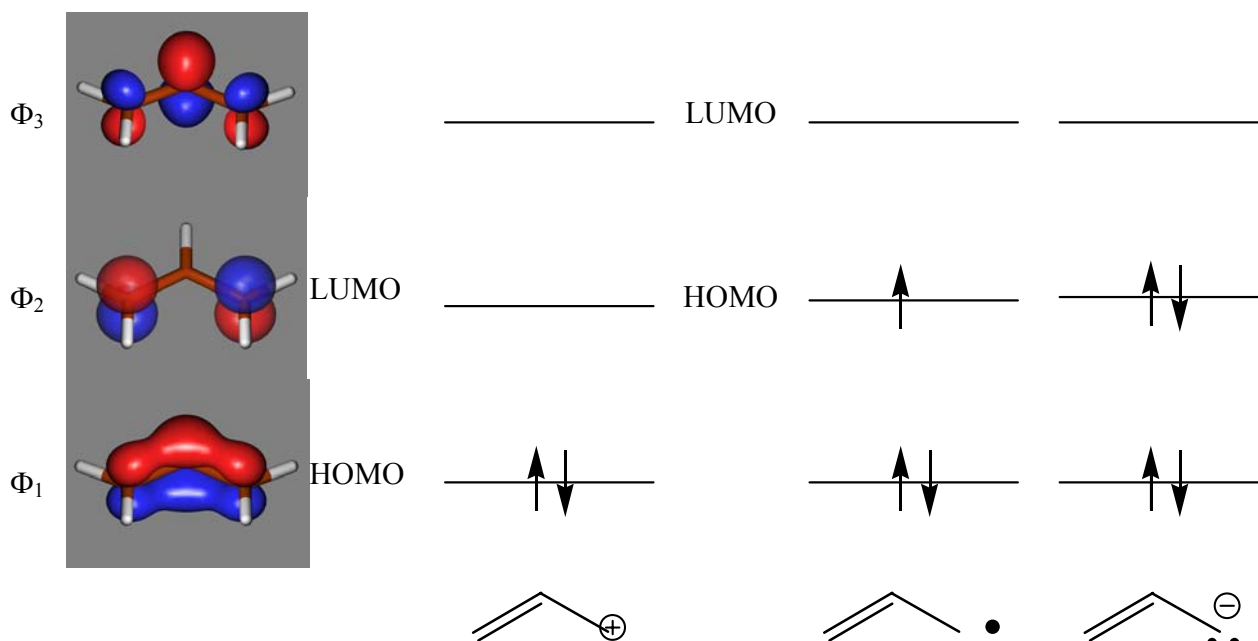


Figure 1.2.1—21. A schematic illustration of the three canonical molecular orbitals, CMO, ϕ_i , and the occupancy scheme of MO energy levels (ϵ_i) of the allyl cation, radical, and anion.

It may be noted that the SHMO method gives an identical set of orbital energies (ϵ_i) for the allyl cation, radical, and anion. This is clearly demonstrated in Figure 1.2.1—21. However, methods that are more sophisticated yield different sets of ϵ_i , in which the cation has the lowest set of MO energies, and the anion has the highest set.

The HOMO and the LUMO assignments are also indicated for the cation and the anion in Figure 1.2.1—21. Note that the occupancy predetermines which orbital will be the HOMO and which one will be the LUMO. Also note that the radical uses the same MO as the anion, but ϕ_2 (i.e. ϵ_2) is only half occupied in the radical, while it is fully occupied in the anion.

The electron density (ρ) can be calculated from the MO coefficients specified in equations 1.2.1-21 and 1.2.1-22. To obtain the density, we need to square the individual coefficients (c_{ij}^2) and multiply them by the occupancy of the i -th MO.

Number of π -electrons contributed by the j -th AO to the i -th MO:

$${}^j\rho_{ii} = n_i c_{ij}^2$$

1.2.1-21. eq

Number of π -electrons in the i -th MO:

$$\rho_{ii} = n_i \sum_j c_{ij}^2$$

1.2.1-22. eq

Number of π -electrons on the j -th AO:

$${}^j\rho = \sum_i n_i c_{ij}^2$$

1.2.1-23. eq

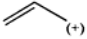
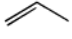
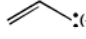
Total number of π -electrons in the molecule:

$$\rho = \sum_i n_i \sum_j c_{ij}^2$$

1.2.1-24. eq

These numbers are given for allyl systems in Table 1.2.1-1.

Table 1.2.1-1 Calculation of π -electron density and net charges for three allyl systems from the LCAO coefficients.

Density from ϕ_i	 $n_1=2$				 $n_1=2, n_2=1$				 $n_1=n_2=2$			
	c^1	c^2	c^3	Total	c^1	c^2	c^3	Total	c^1	c^2	c^3	Total
	${}^1\rho_{ii}$	${}^2\rho_{ii}$	${}^3\rho_{ii}$	ρ_{ii}	${}^1\rho_{ii}$	${}^2\rho_{ii}$	${}^3\rho_{ii}$	ρ_{ii}	${}^1\rho_{ii}$	${}^2\rho_{ii}$	${}^3\rho_{ii}$	ρ_{ii}
from ϕ_3	-	-	-	0.0	-	-	-	0.0	-	-	-	0.0
from ϕ_2	-	-	-	0.0	0.5	0.0	.05	1.0	1.0	0.0	1.0	2.0
from ϕ_1	0.5	1.0	0.5	2.0	0.5	1.0	0.5	2.0	0.5	1.0	0.5	2.0
Density on atom j ${}^j\rho$	0.5	1.0	0.5		1.0	1.0	1.0		1.5	1.0	1.5	
Total π density ρ	2.0				3.0				4.0			
Net charge δ_j	+0.5	0.0	+0.5		0.0	0.0	0.0		-0.5	-0.5	-0.5	

Note that the AO number (j) is the same as the number of atoms, because each atom contributes only one AO ($2p_z$) to the π -MO system.

The net charge (δ), associated with the j -th atom, is calculated from the effective nuclear charge (Z_{eff}), which is 1 for carbon in a π -system, and the electron density. Note that Z_{eff} represents a positive electrostatic charge, while ρ represents a negative electrostatic charge.

$$\delta_j = Z_{\text{eff}}^{-j} \rho$$

1.2.1-25. eq

The δ_j values are given in the last line of Table 1.2.1-1 and shown in Figure 1.2.1—22. This figure also indicates, using dotted lines, that the π -allylic system is fully delocalized.

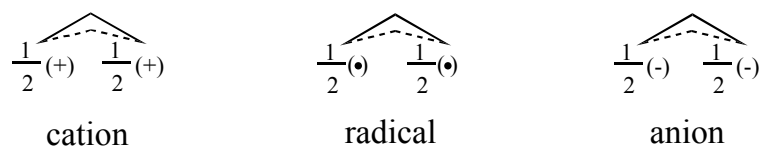


Figure 1.2.1—22 Delocalized π -electron distribution in the allyl cation, radical, and anion.

The π -electron densities associated with the three CMOs (ϕ_1 , ϕ_2 , and ϕ_3) are shown in Figure 1.2.1—23.

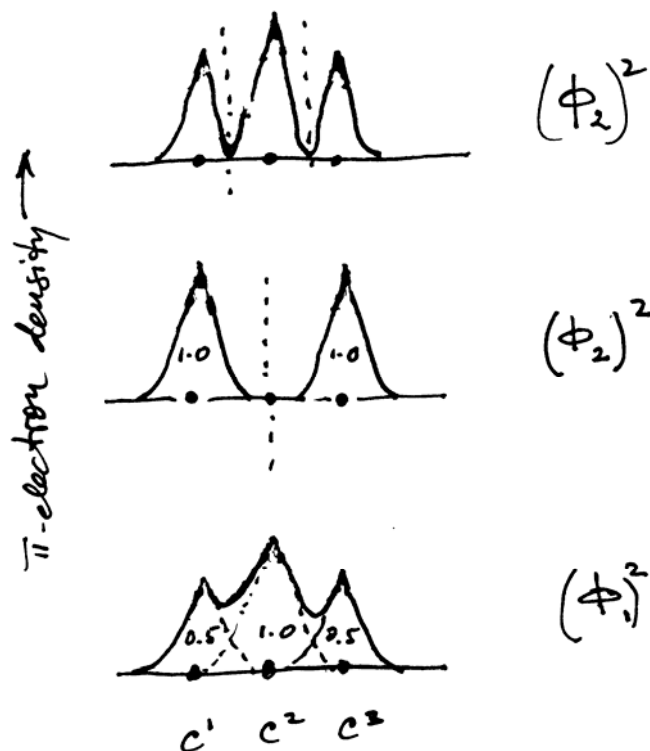
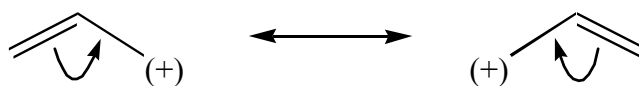


Figure 1.2.1—23 A schematic representation of the contribution to π -electron density by each of the three doubly occupied CMO. Note that at the location of the nodal plane (denoted by dotted line), the density assumes a zero value in ϕ_2^2 and ϕ_3^2 .

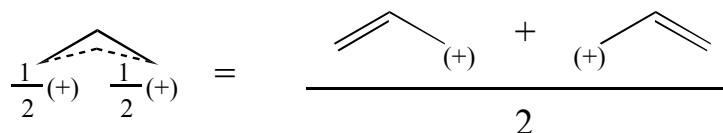
For the allyl cation, only $(\phi_1)^2$ makes a contribution, doing so in the form of $2(\phi_1)^2$. For the allyl anion, the total π -density is $2(\phi_1)^2 + 2(\phi_2)^2$. In contrast to this, for the allyl radical the total π -density is $2(\phi_1)^2 + (\phi_2)^2$. The number under each curve associated with $(\phi_1)^2$ and $(\phi_2)^2$ in Figure 1.2.1—23 corresponds to the numbers given in the first two lines of the allyl anion in Table 1.2.1-1 (ie. to the squares of the LCAO coefficients which measure the number of π -electrons). These numbers effectively represent the area underneath the curves in Figure 1.2.1—23.

Resonance Description of the Allyl Cation, Radical, and Anion

In accordance to MO Theory, Resonance Theory gives an identical charge distribution to the allyl cation, radical, and anion (c.f. Figure 1.2.1—22). This is illustrated below for the allyl cation,

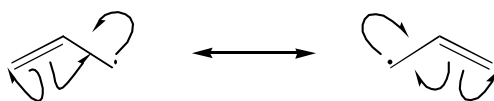


1.2.1-26. eq

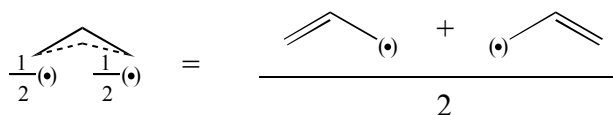


1.2.1-27. eq.

the allyl radical

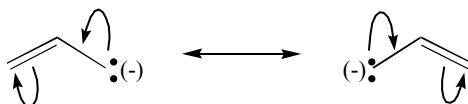


1.2.1-28. eq

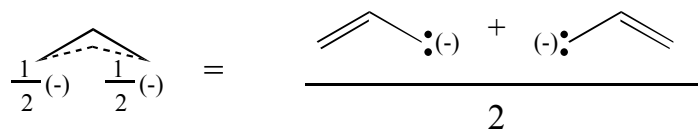


1.2.1-29. eq

and the allyl anion:



1.2.1-30. eq



1.2.1-31. eq

The equal distribution of charge (i.e. electrons) on the two terminal carbons suggests that these are the reaction sites. The cation reacts with a nucleophile, the radical with another radical, and the anion with an electrophile. This will be discussed later in this chapter. It might be added that while the allyl cations, and allyl radicals occur quite frequently, allyl anions, do not play a prominent role. However, when a heteroatom is placed in the allylic position, an allyl anion electron configuration can be achieved. This is the case with enols (Figure 1.2.1—24 a) and enamines (Figure 1.2.1—24 b), which will be further discussed.

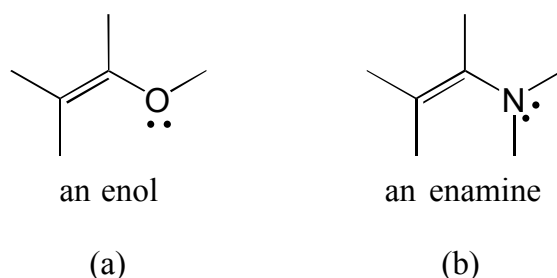
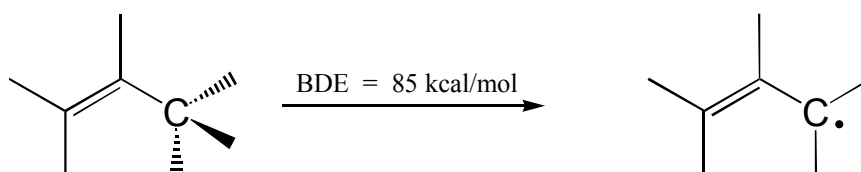


Figure 1.2.1—24. The Allyl Radical and the Allyl Cation as Reaction Intermediates.

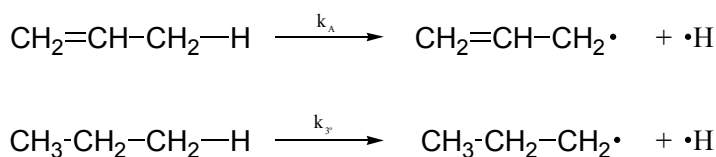
One of the weakest C-H bonds is the allylic C-H, which is easily broken.



1.2.1-32. eq.

As you can see, the BDE (85 kcal/mole) for the allylic C-H is lower than that for 1^o, 2^o, and 3^o C-H bonds (98, 94.5 and 91 kcal/mole, respectively).

Though for the parent allyl radical (H₂C=CH-CH₂·), the radical is a 1^o carbon, it is 6 kcal/mol more stable than a genuine 1^o carbon such as (H₃C-CH₂-CH₂·). This 6 kcal/mol difference does not seem to be very much, but it is significant when it predetermines the rate of a reaction. If these BDE energy values were the activation energies for a reaction,



1.2.1-33. eq.

the relative rates would incorporate these BDE values. Assuming that the frequency factors, to be used in Arrhenius' equation, are nearly the same, they would cancel, and at 300K the value of RT is about 0.6 (i.e. 0.002 x 300 = 0.6)

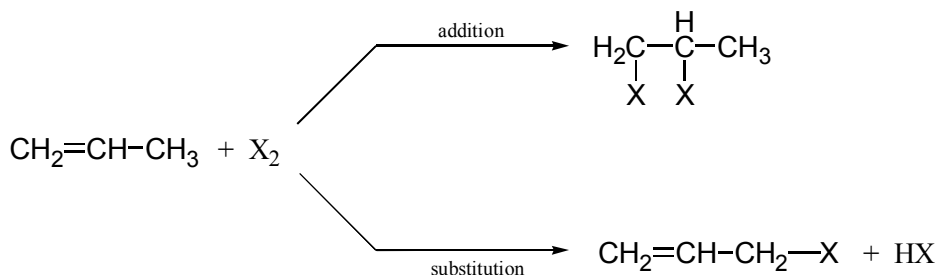
$$\frac{k_A}{k_{1^\circ}} = \frac{A_A}{A_{1^\circ}} \frac{e^{-85/RT}}{e^{-91/RT}} \approx e^{-(85-91)/0.6} = e^{+6/0.6} = e^{10} = 22,026.5$$

1.2.1-34. eq

This implies that the allylic C-H bond is over 22 thousand times more reactive than a 1^o C-H bond. Thus, a 6 kcal/mol energy difference is very significant because it is included in the exponent.

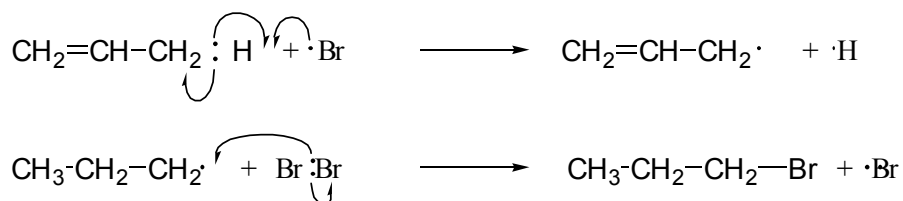
When an allylic system, such as propene, is reacted with a halogen, two reactions (addition and substitution) compete with each other. Low temperatures favor addition, while high temperatures favor

substitution. It should be noted that high concentrations favor addition, while low concentrations favor substitution.¹



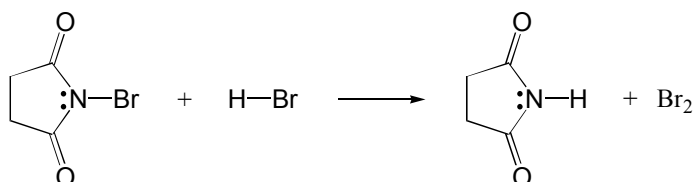
1.2.1-35. eq.

The mechanisms of the chain propagation step of free radical substitution are the same as that of methane halogenation.²



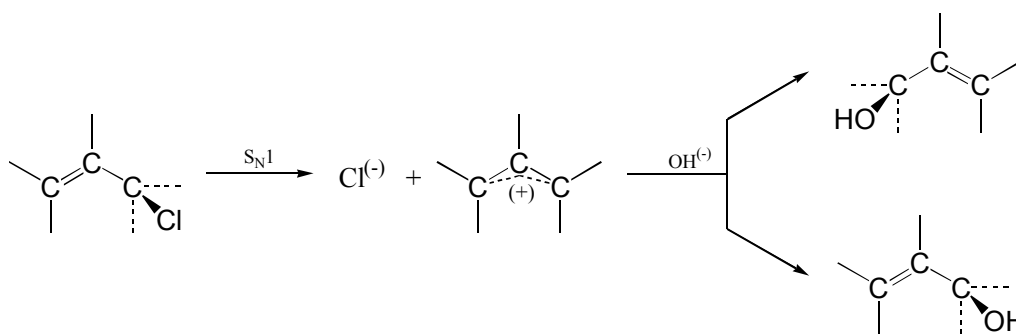
1.2.1-36. eq.

However, in order to guarantee a low Br_2 concentration, N-bromo succinamide (NBS), instead of elemental Br_2 , is used as the bromine source.



1.2.1-37. eq.

The allyl radical is an intermediate in the halogenation reaction (i.e. allylic bromination) as specified by 1.2.1-36. eq.. Once an allylic halide is formed, it may undergo $\text{S}_{\text{N}}1$ substitution, generating an allyl cation as a reaction intermediate.³



1.2.1-38. eq.

The attack of the allyl cation by the OH^- , or by any other nucleophile, can occur at either of the two equivalent terminal carbon atoms.

Needless to say, an allylic cation can be not only 1° , but 2° or 3° as well. The extra allyl substitution in both 2° and 3° enhances the stability of the allyl cation (c.f. Figure 1.2.1—25).

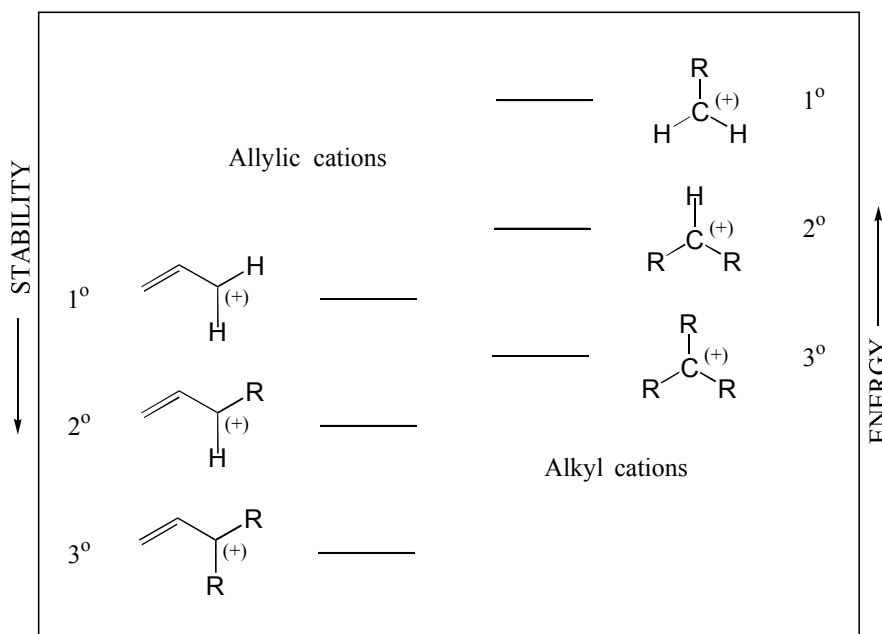
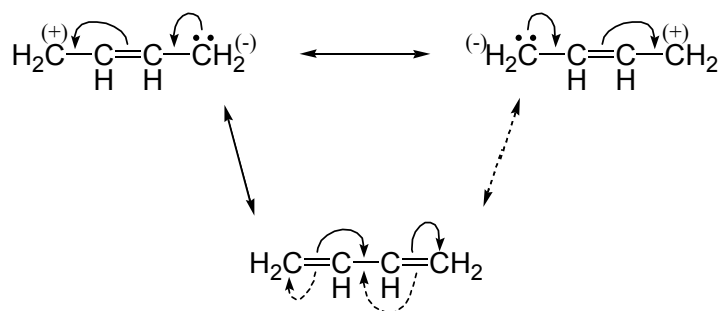


Figure 1.2.1—25 A schematic representation of relative stabilities of a variety of carbocations.

Theories of Conjugative Stabilization: Butadiene

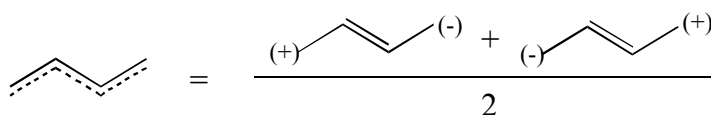
When two carbon-carbon double bonds are in conjugation with one another, they will be stabilized by about 3 to 4 kcal/mol, with respect to their isolated states. Let's use 1,3-butadiene as an example. Resonance Theory suggests the following explanation for conjugative stabilization.



1.2.1-39. eq.

In 1.2.1-39. eq., the curved arrows represent the necessary electron shift to generate the horizontally written ionic resonance structure. In contrast, the curved arrow in 1.2.1-39. eq. relates the one covalent structure at the bottom to the ionic structures at the top (i.e. in 1.2.1-39. eq.).

The contributing resonance structures of 1.2.1-39. eq. suggest that the terminal carbon atoms may be more vulnerable to electrophilic or nucleophilic attack than the two central carbon atoms. However, the average of the two ionic structures in 1.2.1-39. eq. gives a neutral pattern as seen in the contributing resonance structure of 1.2.1-39. eq. This is also illustrated in 1.2.1-40. eq.



1.2.1-40. eq.

Within the MO theory, one needs to consider the AO basis set which consists of four unhybridized $2p_z$ atomic orbitals as shown in Figure 1.2.1—26

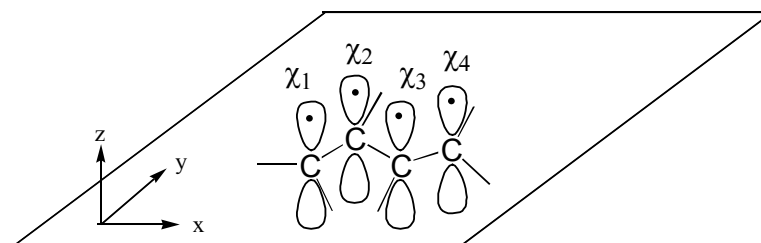


Figure 1.2.1—26 A schematic illustration of the geometry of 1,3-butadiene, showing the four unhybridized $2p_z$ AO (χ_j) from which the π -type MO (ϕ_i) is constructed by the LCAO method.

Figure 1.2.1—26 also shows that the four carbon atoms contribute four electrons to the π -system. This leads to two doubly occupied MOs, as has been demonstrated in the first chapter (c.f. Figure 1.2.1—28)

The LCAO expansion of the four π -type CMOs associated with 1,3-butadiene is as follows

$$\phi_1 = 0.372\chi_1 + 0.601\chi_2 + 0.601\chi_3 + 0.372\chi_4$$

1.2.1-41. eq.

$$\phi_2 = 0.601\chi_1 + 0.372\chi_2 - 0.372\chi_3 - 0.601\chi_4$$

1.2.1-42. eq.

$$\phi_3 = 0.601\chi_1 - 0.372\chi_2 - 0.372\chi_3 + 0.601\chi_4$$

1.2.1-43. eq.

$$\phi_4 = 0.372\chi_1 - 0.601\chi_2 + 0.601\chi_3 - 0.372\chi_4$$

1.2.1-44. eq.

As in the case of the allyl system, we can rewrite 1.2.1-41. eq. in linear algebraic form analogous to 1.2.1-15. eq. - 1.2.1-17. eq. and 1.2.1-18. eq.

$$\begin{pmatrix} \phi_1 \\ \phi_2 \\ \phi_3 \\ \phi_4 \end{pmatrix} = \begin{pmatrix} 0.372 & 0.601 & 0.601 & 0.372 \\ 0.601 & 0.372 & -0.372 & -0.601 \\ 0.601 & -0.372 & -0.372 & -0.601 \\ 0.372 & -0.601 & -0.601 & -0.372 \end{pmatrix} \begin{pmatrix} \chi_1 \\ \chi_2 \\ \chi_3 \\ \chi_4 \end{pmatrix}$$

1.2.1-45. eq.

$$\phi = \mathbf{C}\chi$$

1.2.1-46. eq.

Equation 1.2.1-41. eq. may also be presented in a short hand notation:

$$\phi_i = \sum_{j=1}^4 c_{ij} \chi_j$$

1.2.1-47. eq.

Table 1.2.1-2. Calculation of π -electron density and net charges for 1,3-butadiene from the LCAO coefficients.

Density from ϕ_i	c^1 $^1\rho_{ii}$	c^2 $^2\rho_{ii}$	c^3 $^3\rho_{ii}$	c^4 $^4\rho_{ii}$	Total ρ_{ii}
from ϕ_4	-	-	-	-	0.0
from ϕ_3 (LUMO)	-	-	-	-	0.0
from ϕ_2 (HOMO)	0.723	0.277	0.277	0.723	2.0
from ϕ_1	0.277	0.723	0.723	0.277	2.0
Total	1.000	1.000	1.000	1.000	4.0
Net charge	0.000	0.000	0.000	0.000	

The π -electron densities associated with the two doubly occupied CMO (ϕ_1 and ϕ_2) are shown in Figure 1.2.1—27. This figure is analogous to Figure 1.2.1—24. drawn for the allyl system. However, in

this case, only the doubly occupied CMOs are shown, both of which contribute to the total electron density: $2(\phi_1)^2 + 2(\phi_2)^2$.

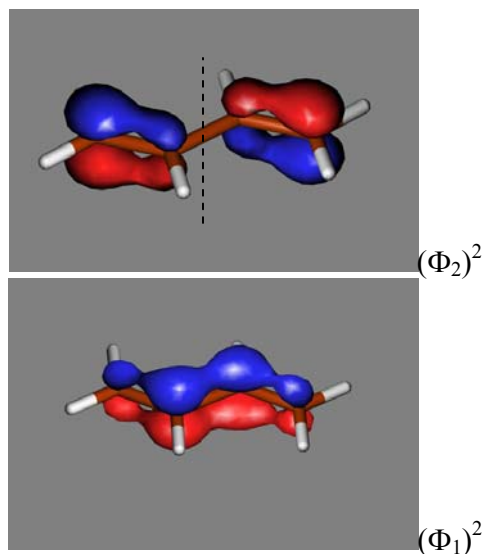


Figure 1.2.1—27 A schematic representation of the contribution to π -electron density by each of the two doubly occupied CMOs. Note that at the location of the nodal plane (denoted by a dotted line) of ϕ_2 , the density of the second MO assumes zero value.

Not only hydrocarbons may have conjugated systems. We can envision a number of cases with heteroatoms such as oxygen and nitrogen.



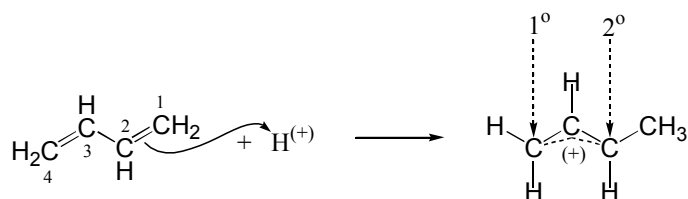
1.2.1-48. eq.



1.2.1-49. eq.

Electrophilic Addition to Conjugated Dienes

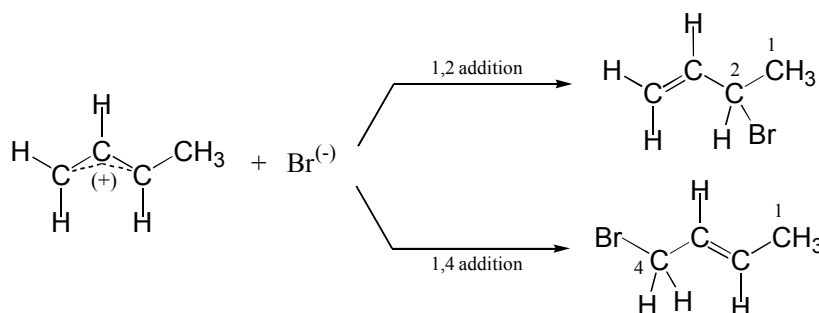
Electrophilic addition to a conjugated diene, like 1,3-butadiene, leads to an allylic cation intermediate. The proton adds to the terminal carbon since the HOMO density, $(\Phi_2)^2$, as shown in Figure 1.2.1—27 and the Table 1.2.1-2, is the highest.



1.2.1-50. eq.

As shown in Table 1.2.1-1 and Figure 1.2.1—22 the unsubstituted allyl cation, which is similar of the substituted intermediate shown in 1.2.1-50. eq. has the highest net positive charge at the two terminal carbon.

The left-hand side terminal carbon of the intermediate allylic system is 1° , and the right-hand side carbon of the allylic system is 2° . As a result, the two carbons will be vulnerable to nucleophilic attack to somewhat different degrees. Furthermore, nucleophilic attack at the 2° carbon leads to a 1,2-addition product, while nucleophilic attack at the 1° carbon leads to 1,4-addition product.



1.2.1-51. eq.

The latter product, 1.2.1-51. eq. (b), is expected to be more stable than the former 1.2.1-51. eq. (a). This is due to the latter product (b) having two R-groups attached to the olefinic double bond, while in the former (a), there is only one R-group substituted. Thus the 1,4-addition product would be thermodynamically favored. The reaction yields a mixture of the two isomers, but their product ratio depends on the temperature of the reaction.

Table 1.2.1-3. Percentage of addition products of the $\text{H}_2\text{C}=\text{CH}-\text{CH}=\text{CH}_2 + \text{HBr}$ reaction observed at two different temperatures.

Reaction	$\text{H}_2\text{C}=\text{CH}-\text{CHBr}-\text{CH}_3$	$\text{BrH}_2\text{C}-\text{CH}=\text{CH}-\text{CH}_3$
temp.	1,2 adduct	1,4 adduct
-80 °C	80%	20%
+40 °C	20%	80%

At a higher temperature (e.g. at 40 °C), the 80%: 20% reaction mixture obtained at -80 °C rearranges to a 20%: 80% product ratio.

The energy profile for this reaction is depicted in Figure 1.2.1—28. As you can see, the barrier, which must be overcome to give the most stable product (the 1,4-adduct), is the highest of the two

barriers in the right half of the energy profile. Consequently, at a low temperature, it is much easier for the system to overcome the lower barrier, giving the least stable product (the 1,2-adduct). Thus, it is obvious that at a low temperature, the relative stability of the transition states predetermines the product ratio. This is called kinetic control. However, at a higher temperature, the system has enough energy to overcome both barriers. As a result, the allylic intermediate can lead to the 1,2- or the 1,4-adduct. As well, at a higher temperature, the 1,2-adduct can revert back to the allylic intermediate, which preferentially forms the 1,4-adduct because it is the most stable product. Thus, at a higher temperature, the relative stability of the products predetermines the product ratio. This is called thermodynamic control.

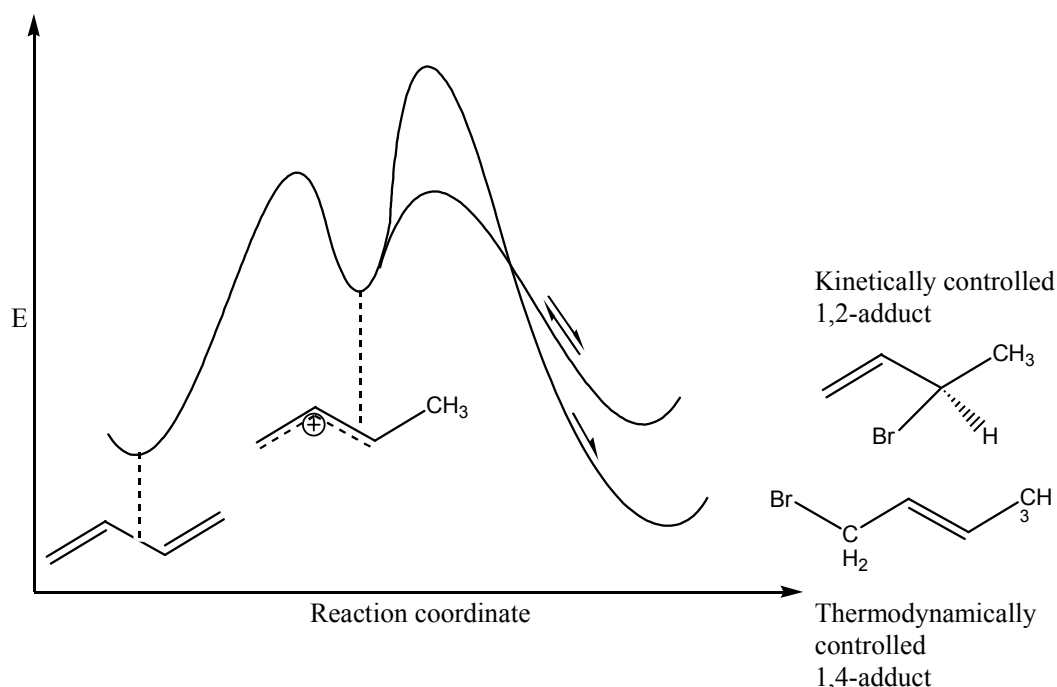


Figure 1.2.1—28 A schematic representation of the energy profile for the 1,2- and 1,4- addition of HBr to 1,3-butadiene. (See appendix 1)

1.2.2 Schrödinger equation and Hamiltonian operators

The Schrödinger wave equation 1.2.2-1. eq. encompasses all the chemistry of a given molecular system.

$$\hat{H}(1,2,3,\dots)\Psi(1,2,3,\dots) = E(1,2,3,\dots)\Psi(1,2,3,\dots)$$

$$\begin{array}{c} \downarrow \text{Variation theorem} \\ \left. \begin{array}{l} \hat{F}\phi_1 = \varepsilon_{11}\phi_1 \\ \hat{F}\phi_2 = \varepsilon_{22}\phi_2 \\ \cdot \\ \cdot \\ \hat{F}\phi_M = \varepsilon_{MM}\phi_M \\ \cdot \\ \cdot \\ \hat{F}\phi_N = \varepsilon_{NN}\phi_N \end{array} \right\} \text{Fock wave equations} \end{array}$$

1.2.2-1. eq.

The many-electron Hamiltonian operator, $\hat{H}(1, 2, 3, \dots)$, describes all the electrostatic interactions for all the electrons in the field of the atomic nuclei that make up the molecule. The many-electron wave functions, $\Psi(1, 2, 3, \dots)$, describes the simultaneous distribution of all the electrons (denoted as 1,2,3,...) in the field of the atomic nuclei. The many-electron Hamiltonian and the many-electron wave functions can be used to calculate the total energy, $E(1, 2, 3, \dots)$ for the many-electron system, which includes both the kinetic energy (KE) and the potential energy (PE) components.

The Central Field Hamiltonians

The hydrogen atom is a simple mathematical problem in quantum mechanics but for any atom with more than one electron an exact solution is impossible. A good starting point is provided by assuming that each electron moves in a central or spherically symmetric force field produced by the nucleus and the other electrons. The instantaneous action of all the electrons of an atom on one of their number is replaced by the averaged charge distribution of each other electron. This charge distribution summed over the electrons of an atom is very nearly spherically symmetrical and in the central field approximation, one takes a spherical average.

In the one electron central field problem (the hydrogen atom), the Schrödinger equation in CGS units is:

$$\left\{ -\frac{\hbar^2}{8\pi^2 m_0} \nabla^2 - \frac{e^2}{r} \right\} \Psi = E\Psi$$

1.2.2-2. eq.

where ∇^2 is the Laplacian operator

$$\nabla^2 = \frac{\partial^2}{\partial x^2} + \frac{\partial^2}{\partial y^2} + \frac{\partial^2}{\partial z^2}$$

1.2.2-3. eq.

Utilizing the definition of atomic units of distance and energy the conversion leads to a very simple expression for the Hamiltonian operator of the hydrogen atom in a.u.

$$\hat{H}^{a.u.} = -\frac{1}{2}\nabla^2 - \frac{1}{r}$$

1.2.2-4. eq.

The first term represents the kinetic energy (KE) and the second term is the potential energy (PE) of the electron.

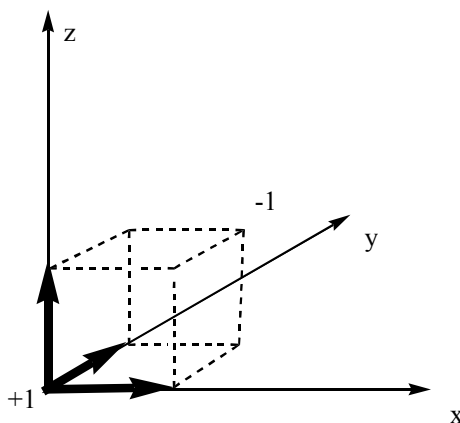
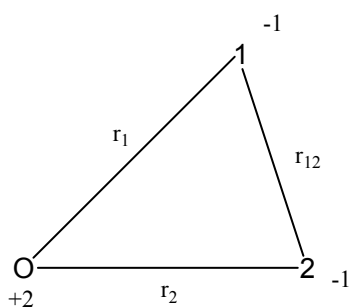
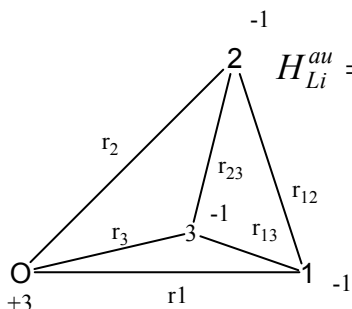


Figure 1.2.2—1 Hydrogen atom in Cartesian coordinate system with charges and distances in atomic units.

The Hamiltonian operator for other atomic system (e.g. He, Li) can also be written in a correspondingly simple form in a.u. as illustrated in Figure 1.2.2—2. A new type of interaction, the electron-electron repulsion represented by $1/r_{ij}$ (and the cause of previously discussed difficulties in exactly solving many electron problems) has entered into the Hamiltonian, which of course was not represented in the one electron case.



$$H_{He}^{au} = \underbrace{-\frac{\nabla_1^2}{2} - \frac{\nabla_2^2}{2}}_{\text{K.E.}} - \underbrace{\frac{2}{r_1} - \frac{2}{r_2} + \frac{1}{r_{12}}}_{\text{P.E.}}$$



$$H_{Li}^{au} = \underbrace{-\frac{\nabla_1^2}{2} - \frac{\nabla_2^2}{2} - \frac{\nabla_3^2}{2}}_{\text{K.E.}} - \underbrace{\frac{3}{r_1} - \frac{3}{r_2} - \frac{3}{r_3} + \frac{1}{r_{12}} + \frac{1}{r_{13}} + \frac{1}{r_{23}}}_{\text{P.E.}}$$

all electrons all electrons all pairs

Many electron atom

$$H_{Atom}^{au} = \underbrace{-\sum_i \frac{\nabla_i^2}{2}}_{\text{K.E.}} + \underbrace{\sum_i -\frac{Z}{r_i} + \sum_{i,j} \frac{1}{r_{ij}}}_{\text{P.E.}}$$

Figure 1.2.2—2 Hamiltonian operators for atomic systems

The Molecular Hamiltonian

The nonrelativistic Hamiltonian operator for a molecule of N nuclei and n electrons is:

$$\hat{H} = \underbrace{-\frac{1}{2} \sum_{k=1}^N \frac{1}{M_k} \nabla_k^2}_1 - \underbrace{\frac{1}{2} \sum_{\mu=1}^n \nabla_{\mu}^2}_2 - \underbrace{\sum_{\mu=1}^n \sum_{k=1}^N \frac{z_k}{r_{\mu k}}}_3 + \underbrace{\sum_{\mu < \nu}^N \frac{1}{r_{\mu \nu}}}_4 + \underbrace{\sum_{k < l}^N \frac{z_k z_l}{r_{kl}}}_5$$

1.2.2-5. eq.

All nuclear and electronic coordinates are referred to the centre of mass of the system. The various terms are (1.) the kinetic energy of the nuclei where M_K is the mass in atomic units of the k^{th} nucleus (2.) the kinetic energy of the electrons. (3) the electron-nucleus-attractive potential energy (4.) electron-electron-repulsive potential energy and (5.), the nuclear-nuclear repulsive potential energy.

1.2.3 A Born-Oppenheimer Approximation and concept of Potential Energy Surfaces (PES)

The total system can be described by the total Schrödinger Equation

$$\hat{H}_{total} \Psi_{total} = E_{total} \Psi_{total}$$

1.2.3-1. eq.

If Ψ_{total} is a real (rather than complex) function then we may pre-multiply both side of 1.2.3-1. eq. by Ψ_{total} and integrate over all coordinates denoted by $d\tau_{total}$

$$\int_{total} \Psi_{total} \hat{H}_{total} \Psi_{total} d\tau_{total} = E_{total} \underbrace{\int_{total} \Psi_{total} \Psi_{total} d\tau_{total}}_{=1 \text{ if wavefunction is normalised}}$$

1.2.3-2. eq.

Consequently

$$E_{total} = \int_{total} \Psi_{total} \hat{H}_{total} \Psi_{total} d\tau_{total}$$

1.2.3-3. eq

The total Hamiltonian is consists of two components

$$\hat{H}_{total} = \hat{H}_{nuclear} + \hat{H}_{electronic}$$

1.2.3-4. eq

The Born–Oppenheimer approximates separates the nuclear and electronic motions (coordinates) which leads to the arithmetic product of an electronic and a nuclear wave function.

$$\Psi_{total} = \Psi_{nucl} \Psi_{elect.}$$

1.2.3-5. eq.

substituting 1.2.3-4. eq and 1.2.3-5. eq. into 1.2.3-3. eq we obtain the following:

$$E_{total} = \int \int_{nucl\ elect.} \Psi_{nucl} \Psi_{elect.} (\hat{H}_{nucl} + \hat{H}_{elect}) \Psi_{nucl} \Psi_{elect.} d\tau_{nucl} d\tau_{elect}$$

1.2.3-6. eq

$$E_{total} = \int_{nucl} \Psi_{nucl} \hat{H}_{nucl} \Psi_{nucl} d\tau_{nucl} \underbrace{\int_{elect} \Psi_{elect} \Psi_{elect} d\tau_{elect}}_{=1\text{ if normalized}} + \int_{elect} \Psi_{elect} \hat{H}_{elect} \Psi_{elect} d\tau_{elect} \underbrace{\int_{nucl} \Psi_{nucl} \Psi_{nucl} d\tau_{nucl}}_{=1\text{ if normalized}}$$

1.2.3-7. eq

$$E_{total} = \underbrace{\int_{nucl} \Psi_{nucl} \hat{H}_{nucl} \Psi_{nucl} d\tau_{nucl}}_{E_{nucl}} + \underbrace{\int_{elect} \Psi_{elect} \hat{H}_{elect} \Psi_{elect} d\tau_{elect}}_{E_{elect}}$$

1.2.3-8. eq

$$E_{total} = E_{nucl} + E_{elect}$$

1.2.3-9. eq

Thus the separation of the nuclear and electronic coordinates leads to two separate wave equations, an electronic wave equation and a nuclear wave equation

$$\hat{H}_{electr} \Psi_{electr} = E_{electr} \Psi_{electr}$$

We solve this first
for a fixed nucleus
arrangement



$$\hat{H}_{nucl} \Psi_{nucl} = E_{nucl} \Psi_{nucl}$$

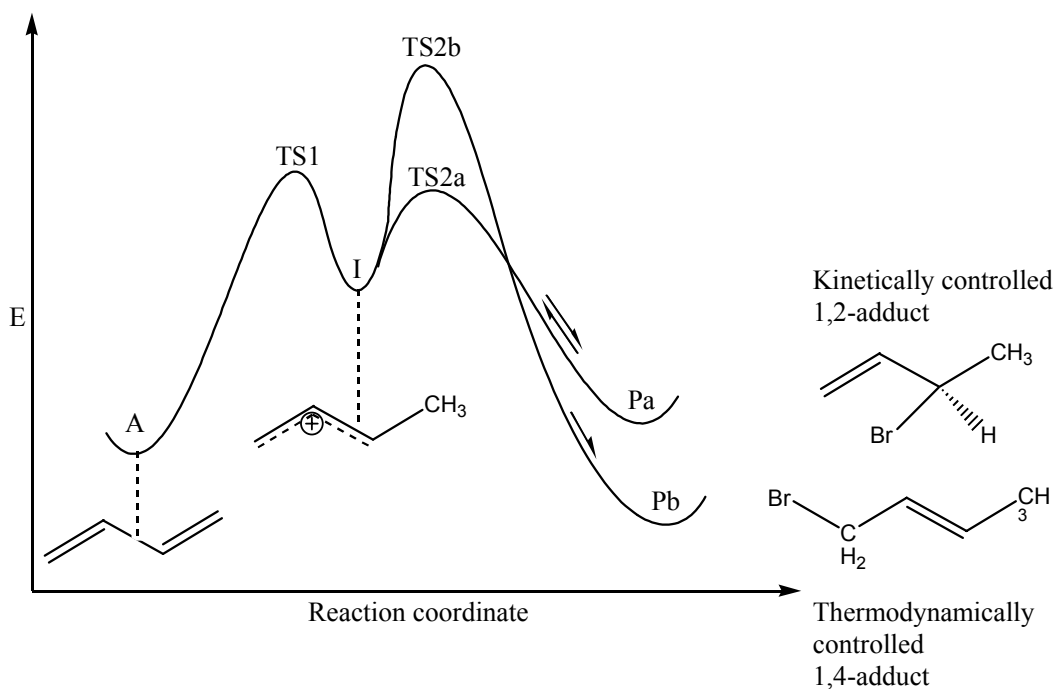
We solve this subsequently
for a variable nuclear
arrangement to see
molecular vibration

1.2.3-10. eq

Appendix

Appendix 1

Problem: Calculate the energy of each step in the 1,2- and 1,4- addition of HBr to 1,3-butadiene the reaction.



Solution: input file for calculate the energy of (I)

```
%chk=I.chk
%mem=6MW
%nproc=1
#p opt=gdiis hf/3-21g geom=connectivity

optimization of ( I ) of butadiene brom addition
```

```
1 1
C      -2.21115567   -2.21324441   0.05171052
H      -3.07828531   -2.84002569   0.06317449
H      -1.82121943   -1.85640631  -0.87862077
C      -1.60677309   -1.87134597   1.21549495
H      -0.73962680   -1.24458777   1.20402910
C      -2.16799571   -2.38491776   2.55447709
H      -3.03514083   -3.01167758   2.56594280
C      -1.48116521   -1.99644128   3.87695579
```

H	-2.00637110	-2.44186088	4.69589422
H	-0.46979013	-2.34567840	3.86961604
H	-1.49012122	-0.93186917	3.98422179

```

1 2 1.0 3 1.0 4 1.5
2
3
4 5 1.0 6 1.5
5
6 7 1.0 8 1.0
7
8 9 1.0 10 1.0 11 1.0
9
10
11

```

Species	Energy in a.u.
A	-154.05945640
TS1	
I	-154.38425367
TS2a	
TS2b	
Pa	-2714.72484443
Pb	-2714.72445997

The summary section of the output file for Pb:

```

1|1|UNPC-UNK|FOpt|RHF|3-21G|C4H7Br1|PCUSER|06-Oct-2004|0||#P OPT=GDIIS
HF/3-21G GEOM=CONNECTIVITY||optimization of (Pa ) of butadien brom ad
dition||0,1|C,1.3449867126,1.639596148,0.8394679171|H,2.2958178322,1.1
867374241,0.6152529561|C,0.2737920085,0.8808869844,0.9498521243|H,-0.6
849740087,1.3173134446,1.1612936463|C,0.2948578246,-0.6001410453,0.803
6834271|H,-0.1968086211,-1.1051384432,1.6168426719|H,1.2859612719,-0.9
929607411,0.6597790648|C,1.351666284,3.1383525781,1.0027984554|H,2.015
9851708,3.4328594526,1.8094978391|H,1.7072528002,3.6172081943,0.095581
5825|H,0.3597612483,3.513993438,1.2213020271|Br,-0.7535660763,-1.18063
3736,-0.8215531809||Version=x86-Win32-G03RevB.05|State=1-A|HF=-2714.72
446|RMSD=4.075e-009|RMSF=4.059e-006|Dipole=0.5860893,0.5085799,0.73778
32|PG=C01 [X(C4H7Br1)]||@

```

LET US LEARN TO DREAM, GENTLEMEN, THEN PERHAPS WE SHALL
 DISCOVER THE TRUTH; BUT LET US BEWARE OF PUBLISHING
 OUR DREAMS ABROAD BEFORE THEY HAVE BEEN SCRUTINIZED
 BY OUR VIGILANT INTELLECT ... LET US ALWAYS ALLOW
 THE FRUIT TO HANG UNTIL IT IS RIPE. UNRIPE FRUIT
 BRINGS EVEN THE GROWER BUT LITTLE PROFIT; IT DAMAGES
 THE HEALTH OF THOSE WHO CONSUME IT; IT ENDANGERS
 PARTICULARLY THE YOUTH WHO CANNOT YET DISTINGUISH
 BETWEEN RIPE AND UNRIPE FRUIT.

-- KEKULE, 1890

Job cpu time: 0 days 0 hours 2 minutes 26.0 seconds.

File lengths (MBytes): RWF= 11 Int= 0 D2E= 0 Chk= 4 Scr= 1

Normal termination of Gaussian 03 at Wed Oct 06 21:48:33 2004.

Literature

1
2
3